Developments in the design of bulb turbines

By F. Schweiger and J. Gregori, Professor* and Research Scientist**

A research study has been carried out on bulb turbines using data on more than 100 units from various manufacturers and other sources, aimed at providing engineers with reliable and up-to-date statistical information. This work covers most units of this type built up to now, and therefore gives an overview of the present trend in bulb turbine design, although various design methods have been used.

Bulb turbine units have certain advantages in relation to conventional Kaplan turbines. Because of the straight draft tube, the efficiency of the bulb design is higher, and its application is favourable in many cases. Therefore, knowledge of basic hydraulic and geometric design parameters is particularly important for the project engineer. The appropriate selection of these parameters is associated with many economic and design problems. Even the right choice of turbine specific speed is directly related to the available head. The positioning of the bulb turbine has some advantages over the conventional Kaplan turbine as regards the cavitation phenomenon, although there is a certain difference in pressure distribution between the top and the bottom part of the runner. In addition, the use of bulb turbines usually allows for less extensive civil works, reducing the total cost of the plant.

*Faculty of Mechanical Engineering, University of Ljubljana, Murnikova 2, 61000 Ljubljana, Yugoslavia; and **Turboinstitute, Rovšnikova 7, 61210 Ljubljana, Yugoslavia.

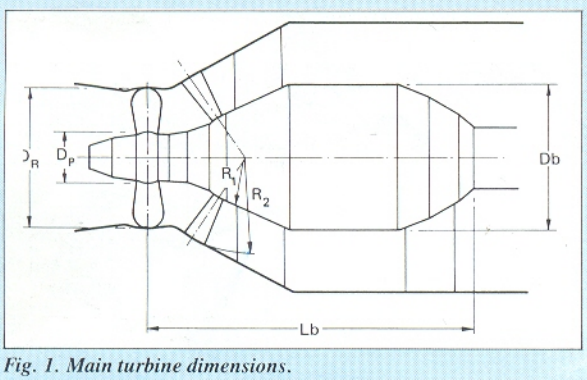

Fig. 1. Main turbine dimensions.

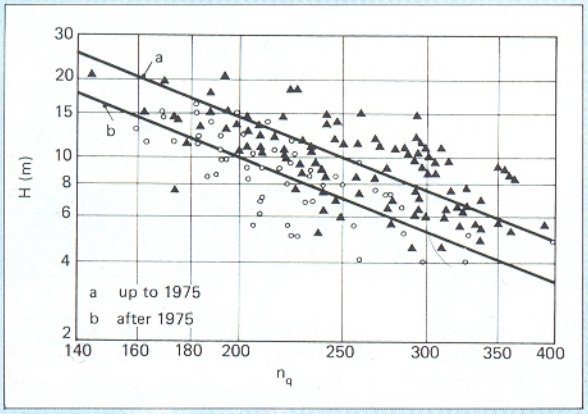

Fig. 2. Head, H, versus specific speed, n_q, with reference to the time of the design.

Technological developments, recent progress in design, and improved manufacturing capability have resulted in the construction of units with larger runner diameters, more advanced shaping, and increased efficiency.

This modern design approach has been to increase specific speed for the same available head (as has been the trend with most turbine types).

To review the latest design methods of different companies and to assist the project engineer with the necessary information, data on bulb units from various sources throughout the world have been collected and evaluated.

Bulb turbine parameters

Bulb turbines cover almost the same range of specific speeds as the Kaplan units, typically within n_q = 140-400. The water turbine is often compared by referring to the specific speed, n_q, and this is expressed by the equation:

$$n_q = n \times Q^{0.5} \times H^{-0.75} \quad \ldots (1)$$

On the basis of data collected and preliminary analyses, a close relationship has been identified between available head, H, and specific speed. This relationship can be expressed as:

$$H = f(n_q) \quad \ldots (2)$$

The analytical relationship of Eq. (2) has proved to be of use as a basis for the project engineer if a new type of turbine unit is being considered.

For more universal application, all the geometric and energy parameters are given in dimensionless form. Generally, the turbine is defined by dimensionless coefficients, as follows (See Fig. 1 for notations):

$$\psi \text{ (energy coefficient)} = gH\,K_\psi^{-1}\,n^{-2}\,D_R^{-2} \quad \ldots (3)$$

$$\phi \text{ (flow coefficient)} = Q\,K_\phi^{-1} n^{-1} D_R^{-3} \quad \ldots (4)$$

Simultaneously, both dimensionless coefficients can be expressed by the specific speed, thus:

$$\psi = f(n_q) \quad \ldots (5)$$

$$\phi = f(n_q) \quad \ldots (6)$$

A similar approach is used for the geometric parameters with dimensionless ratios. On the basis of available data, the following relationships are derived:

$$\frac{D_P}{D_R} = f(n_q) \quad \ldots (7)$$

$$\frac{R_1}{D_R}; \frac{R_2}{D_R} = f(n_q) \quad \ldots (8)$$

$$\frac{D_b}{D_R}; \frac{L_b}{D_R} = f(n_q) \quad \ldots (9)$$

For the turbine runner diameter calculation, the coefficient of peripheral velocity is introduced:

$$K_U = (\pi D_R\, n)\,(2\,gH)^{-0.5} \times 60^{-1} \quad \ldots (10)$$

and eventually expressed by the specific speed:

$$K_U = f(n_q) \quad \ldots (11)$$

Data analysis

The hydraulic and geometric parameters collected by the authors have been used as a basis for the statistical evaluation and presentation of the graphs (Figs. 2-9). The data obtained cover machines built between 1966 and 1985. Preliminary analysis shows the formation of principal groups of data points, pertaining to different time periods. The data were therefore divided into two sets, according to the design date of the turbine, as the statistical analysis could otherwise give misleading results because the information covers too long a period of time. To include an up-to-date computer design approach for the development of turbine units, the data pertaining to $H = f(n_q)$ have been split into two time periods, from 1966 to 1975 and from 1976 to 1985.

On this basis, a statistical evaluation has been made, and two regression characteristics, linking the head, H, and specific speed, n_q, have been established:

- *1966 to 1975*

$$H = 47860\, n_q^{-1.6} \quad \ldots (12)$$

$r = -56$ per cent, standard deviation = 3.855

- *1976 to 1985*

$$H = 69180\, n_q^{-1.6} \quad \ldots (13)$$

$r = -86.94$ per cent, standard deviation = 3.8027

Both functions are presented in Fig. 2, one for each time period. The curves show a constant increase of specific speed, n_q, at a given head, H. The tendency in future design will be towards turbines with higher specific speeds and increased efficiency. This can be achieved with accurate knowledge of flow and energy conditions throughout the turbine passage and well developed design and technical ability.

For a more detailed study of bulb turbine parameters, dimensionless parameters, which are independent of the size and speed of the runner, have been adopted. Figs. 3 and 4 present the energy ψ and flow ϕ coefficient defined by Eqs. (5) and (6). Analytically, the energy coefficient is expressed as:

$$\psi = 77 n_q^{-1.035} \quad \ldots (14)$$

$r = 95.1$ per cent, standard deviation = 0.0603

The flow coefficient is expressed as:

$$\phi = 0.1075 + 0.00085\, n_q \quad \ldots (15)$$

$r = 86$ per cent, standard deviation = 0.072

The results, presented in analytical or graphical form, can be used to select the most suitable type of turbine of modern design. In addition, the turbine runner diameter can be calculated using Eqs. (14) or (15).

By applying Eq. (10), the peripheral velocity coefficient K_U can be determined and, based on statistical data, its regression function can be found, namely:

$$K_U = 1 + 0.0038\, n_q \quad \ldots (16)$$

$r = 81.75$ per cent, standard deviation = 0.25881

Notations

D	=	diameter (m)
g	=	acceleration caused by gravity (m/s^2)
H	=	head (m)
K	=	constant
L	=	length (m)
n	=	speed (rev/min)
Q	=	flow (m^3/s)
R	=	radius (m)
u	=	peripheral velocity (m/s)
b	=	subscript for the body
p	=	subscript for the hub
q	=	subscript for the specific speed
R	=	subscript for the runner
T	=	subscript for the turbine
U	=	subscript for the peripheral
θ	=	specific diameter constant
σ	=	specific speed constant
ϕ	=	flow coefficient constant
ψ	=	energy coefficient constant

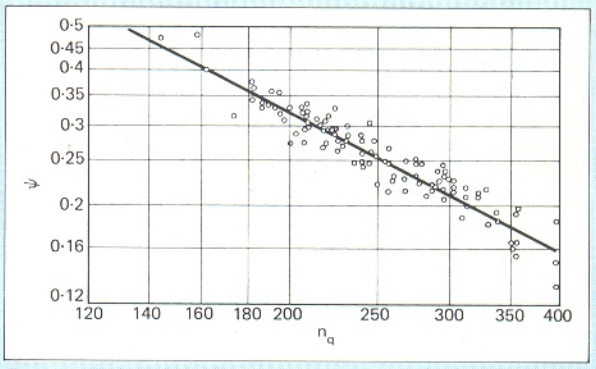

Fig. 3. Energy coefficient, ψ, versus specific speed n_q.

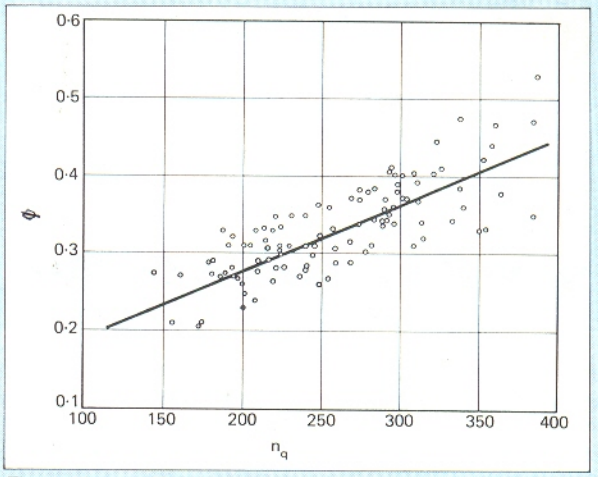

Fig. 4. Flow coefficient, ϕ, versus specific speed n_q.

Graphical presentation of the function $K_U = f(n_q)$ is shown in Fig. 5. By expressing the turbine runner diameter from Eq. (10), its value can be evaluated at a known specific speed. Besides the parameters mentioned above, the geometric parameters are of equal importance to the design engineers. These data have been collected and analysed in accordance with Eqs. (7), (8) and (9). The geometric parameters are expressed

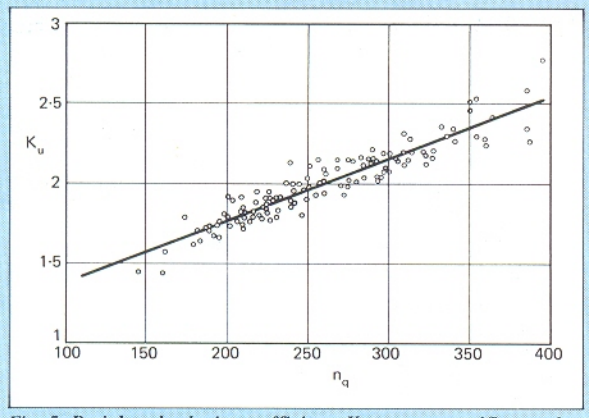

Fig. 5. Peripheral velocity coefficient, K_u, versus specific speed n_q.

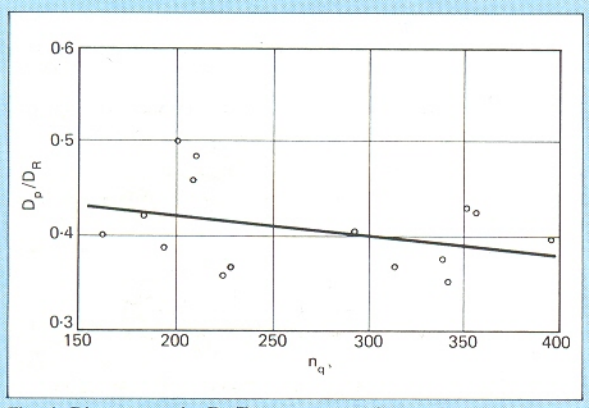

Fig. 6. Diameter ratio, D_p/D_R, versus specic speed n_q.

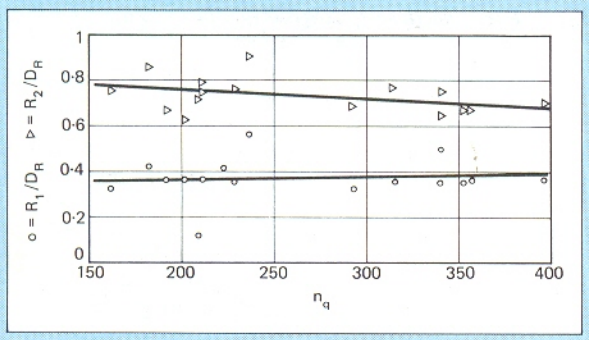

Fig. 7. Radius ratio, R_1/D_R, R_2/D_R, versus specific speed n_q.

in a form of a ratio with the runner diameter, D_R. The analytical relationship is expressed by the following equations:

$$\frac{D_p}{D_R} = 0.443 - 2.2 \times 10^{-4} n_q \qquad \ldots (17)$$

r = 58 per cent, standard deviation = 0.04933

$$\frac{R_1}{D_R} = 0.335 + 1.52 \times 10^{-4} n_q \qquad \ldots (18)$$

r = 55 per cent, standard deviation = 0.09365

$$\frac{R_2}{D_R} = 0.837 - 3.86 \times 10^{-4} n_q \qquad \ldots (19)$$

r = 60 per cent, standard deviation = 0.07873

$$\frac{D_b}{D_R} = 1.143 - 6.8 \times 10^{-4} n_q \qquad \ldots (20)$$

r = 59 per cent, standard deviation = 0.19953

$$\frac{L_b}{D_R} = 2.579 - 0.00123\, n_q \qquad \ldots (21)$$

r = 56 per cent, standard deviation = 0.31336

The graphs from which these equations are derived are shown in Figs. 6, 7 and 8. Although not many geometric data were available, a fair indication of the basic trend of regression functions is given.

Combined results

In this study the hydraulic and geometric parameters have been treated separately. To obtain a more general view of both parameters, it is desirable to join both parameters in dimensionless form. By introducing the specific speed constant, σ_T, as a function of the energy (ψ) and flow (ϕ) (coefficients, the following equation is obtained:

$$\sigma_T = \phi^{0.5} \times \psi^{-0.75} = K_o \times n \times Q^{0.5} (gH)^{-0.75} \qquad \ldots (22)$$

This defines the unit in terms of flow and energy coefficient or of flow and head, accordingly. Using the dimensionless theory and linking the flow and head with the runner geometry, the specific diameter, θ_T, of the machine is obtained, see Eq. 23.

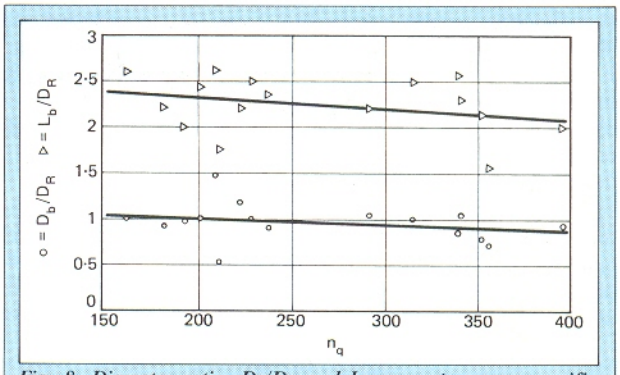

Fig. 8. Diameter ratio, D_b/D_R and L_{b/D_R}, ratio versus specific speed n_q.

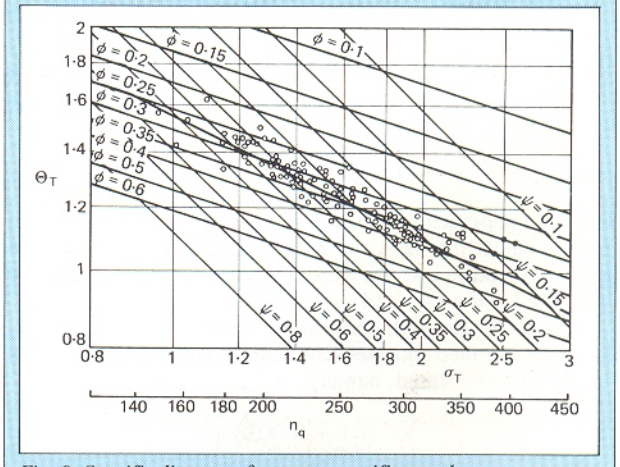

Fig. 9. Specific diameter, θ_t, versus specific speed α_t.

$$\theta_T = \psi^{0.25} \times \phi^{-0.5} = K_\theta D_R (gH)^{0.25} Q^{-0.5}. \quad . \quad . \quad (23)$$

Both parameters σ_T and θ_T present the basic dimensionless coefficients which completely define the turbine unit from the hydraulic and geometric point of view. The evaluation of the coefficients σ_T and θ_T gives a field of points which has to be analysed statistically. The result of this analysis is the regression function $\theta_T = f(\sigma_T)$, shown in Fig. 9, and expressed by the equation:

$$\theta_T = 1.55\, \sigma_T^{-0.5} \quad . \quad . \quad . \quad (24)$$

$r = -84.79$ per cent, standard deviation = 0.1537

Fig. 9 is called a type graph, and presents the optimum statistical data of bulb turbines constructed up to the present. It can be used for calculating the basic runner diameters and to follow the systematic development of the bulb turbines.

Conclusions

This study, together with the data collected and evaluated, can be used for a reliable and quick estimation of basic bulb turbine parameters. It is logical to believe that the regression function with a statistical curve, shown in Fig. 9, yields the average value of the hydraulic and geometric parameters of the best efficiency points pertaining to the individual units.

The type graph is complex, but it is the first systematic approach to linking the basic bulb turbine parameters. In addition, this graph indicates the world trend in the design of these machines. The graph can be used as a statistical pointer to the future design of bulb turbines. □

Acknowledgement

The authors wish to express their thanks to the Research Council of Slovenia for supporting this research work, and to the many companies which supplied data for the study.

Bibliography

SCHWEIGER, F. AND GREGORI J., "Developments in pump-turbines", *Water Power & Dam Construction*; October 1982.
SCHWEIGER, F. AND GREGORI J., "Developments in Francis turbines" *Water Power & Dam Construction*; August 1985.
SCHWEIGER, F. AND GREGORI J. "Developments in the design of Kaplan turbines", *Water Power & Dam Construction*; November 1987.
UEDA, T., "Large capacity bulb units in Japan", *Water Power & Dam Construction*; March 1983.
KOVALEV, N. N., "Projektirovanje gidroturbin", *Mashinostroenie*, Moscow, USSR, 1974.
LOSNIKOVA, A. A., "Vibor parametrov i osnovnih geometričeskih sootnošeni protočnoj česti obratnih gidromašin", *Energomashinostroenie*, Moscow, USSR; 1978.
MOSONYI, E., "Wasserkraftwerke" I and II, VDI Verlag; FRG; 1966.
TAKANORI, Y., "Trends in Hydroelectric Generating Equipment Technology", *Hitachi Review*, Vol. 28 1979.
BUCHI, G., "Turbine Idrauliche", Milan, Italy; 1957.
DAVIS, C. V., "Handbook of Applied Hydraulics", McGraw-Hill, USA; 1970.

Calculation of prototype cavitation characteristics in large bulb turbines

By T. Kubota and T. Tsukamoto, Chief Engineer* and Hydraulic Engineer*

Large bulb turbines have a large vertical span (diameter) between the runner top (the maximum elevation) and bottom (the minimum elevation) compared with the low head that is to be utilized. As the Froude number of a bulb turbine model will not be the same as that of the prototype in most cases, the distribution and development of cavitation at the prototype runner will differ from that observed in the model; cavitation can develop all over the runner (from top to bottom) in the model, but in the prototype the cavitation might only develop around the runner top. A conversion method of the cavitation characteristics from model to prototype has not been established or stipulated in the IEC Code, so far. In this article, the pressure distributions against the vertical distance of a prototype runner is estimated by using: a three-dimensional flow analysis; and the cavitation characteristics observed in model tests.

Using the above, a method is proposed to calculate the cavitation performance of the prototype from model test results.

The application of high specific speed large bulb turbines has been growing along with the recent trend to develop ultra-low head hydroelectric powerplants. When a prototype turbine, which is geometrically similar to the model, is operated under hydrodynamically homologous conditions, its cavitation behaviour is generally considered to be a scaled version of that observed in the model by coinciding the cavitation factor (σ). A large bulb runner will have a large vertical distance (diameter) compared with the low head; however, the effect of gravity (potential head) on the cavitation development will be pronounced. For example, in the First Supplement to Publication 193 (1965) of the IEC Model Test Code[1], it is recommended to consider the Froude similitude when the vertical distance (D) against the net head (H) cannot be ignored ($D > 0.25H$).

*Fuji Electric Co., Ltd. 1-1, Tanabe-Shinden, Kawasaki 210, Japan

Example

Let us consider a low head large bulb turbine with a net head of 5 m and a runner diameter of 7 m as an example. The diameter of the model runner used for the model test would normally be about 0.35 m. When the model Froude number coincides with that of the prototype, the model test head should be less than 0.5 m. Such a low head could not guarantee accurate measurement of the model's performance. To coincide the model cavitation factor with that of the prototype at this low head, the suction head must be less than minus 9 m. If the test loop is exposed to such a large negative pressure, the separation of dissolved air in the water makes it impossible to observe the cavitation accurately. For these reasons, it is difficult to carry out the model test to coincide with the Froude number of the prototype, as the IEC Code recommends.

Experience has shown that it is necessary to increase the test

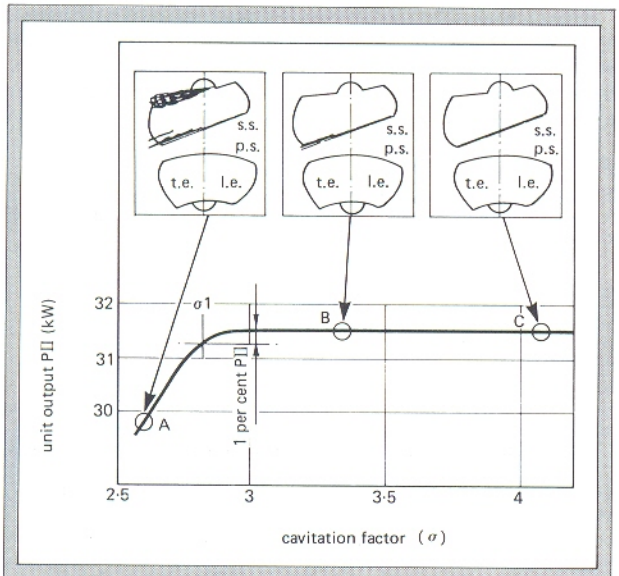

Fig. 1. Cavitation characteristics observed in the model turbine for the New Martinsville powerplant, USA (p.s. = pressure surface, s.s. = suction surface, t.e. = trailing edge, and l.e. = leading edge).

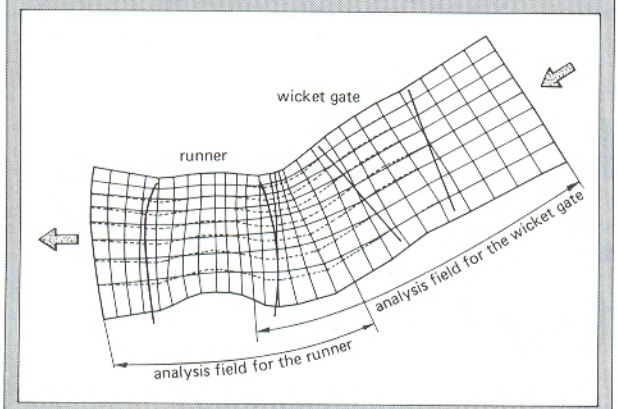

Fig. 2. The meridional streamlines, derived from a three-dimensional analysis, of the flow through the wicket gates and runner of a bulb turbine at New Martinsville powerplant.

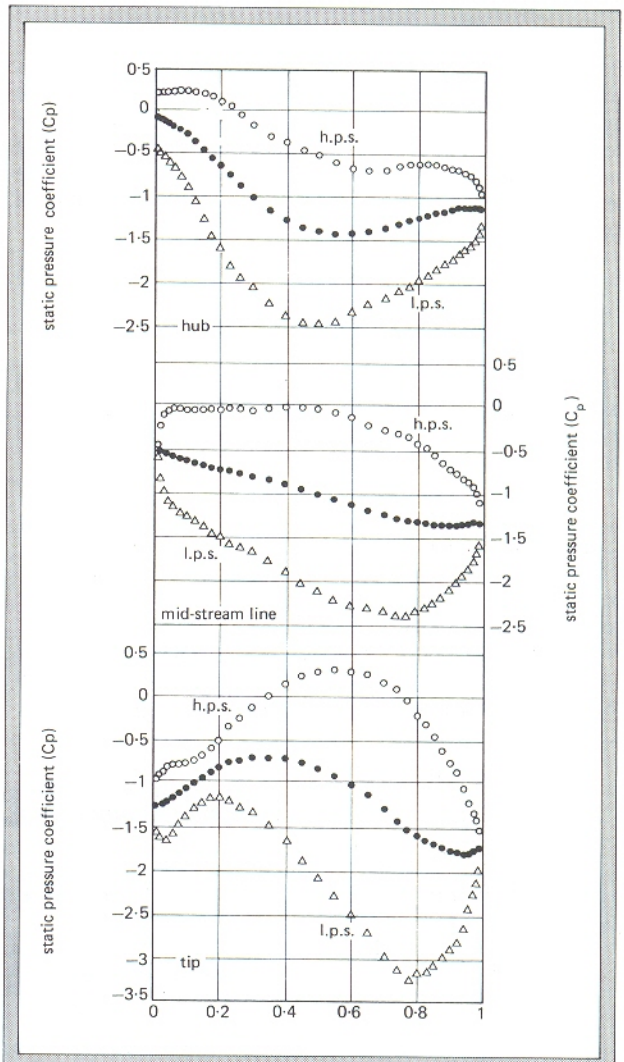

Fig. 3. The distribution of pressure along the blade surface on the runner operating in the turbine shown in Fig. 2. (h.p.s. = high pressure surface and l.p.s. = low pressure surface).

head for cavitation testing against the wide range of σ, while maintaining the accuracy of the model test. Therefore, the model Froude number cannot coincide with that of the prototype. When the model Froude number is different from that of the prototype, the distribution of cavitation development, from the top of the runner to the bottom, becomes different in the prototype from that observed in the model. The cavitation develops almost all over the runner from top to bottom in the model cavitation test, but in the prototype the cavitation develops only around the runner top. No conversion method for these cavitation characteristics has been established so far.

In this report, a numerical analysis is introduced which predicts the vertical pressure distribution throughout the prototype runner by applying a three-dimensional flow analysis to the model test results. Based on the results obtained, a new method is proposed to convert the model cavitation characteristics to the prototype characteristics.

New Martinsville powerplant

The model test was conducted using a model for the low head large bulb turbines of the New Martinsville powerplant (runner diameter 7.3 m, rated net head 5.4 m, rated output power 19 MW) in West Virginia, USA[2]. The model turbine has a runner diameter of 0.365 m and is geometrically homologous to the prototype. Although the model test was carried out under hydraulically homologous conditions, the tested net head was set to 4 m without the Froude number being coincident with the prototype, allowing a highly accurate cavitation performance test.

The model runner diameter of 0.365 m is so small compared with the test head of 4 m that the difference in the cavitation factor between the runner top and bottom was expected, and observed, to be negligible. On the other hand, the cavitation factors at the top and bottom in the prototype runner showed a significant difference. Therefore, in model tests, it is necessary to observe the cavitation development at each elevation of prototype by coinciding the test cavitation factor with the cavitation factor at each elevation of prototype runner.

Fig. 1 shows the unit output ($P11$) versus the cavitation factor (σ); these results were obtained in the model test at the operating point, over the rated output range and under the net head (which is a little lower than the rated head). Typical observation sketches of cavitation development in the model runner are shown in the Figure, with the cavitation factor corresponding to each elevation at which the cavitation factor is 2.6 at the top of the prototype runner. (The reference elevation where the

cavitation factor was obtained was the runner top, the maximum elevation.) At point 'A' in Fig. 1, the cavitation develops rapidly from the top to the bottom of the model runner, resulting in the output deterioration. In the prototype turbines, however, σ becomes point 'B' at the runner centre and point 'C' at the bottom. Since cavitation does not develop at the runner bottom of the prototype, the assumption of a drastic decrease in prototype output is not realistic. Therefore, the model cavitation characteristics must be converted to that of the prototype, taking the above into consideration.

Calculation of pressure distribution

Three-dimensional flow analysis

A three-dimensional flow analysis was performed through the wicket gates and runner of the New Martinsville powerplant as shown in Fig. 2. The flow analysis computer programme [3] is based on the theory by Senoo and Nakase[4,5].

The inlet flow condition to the wicket gates was assumed as uniform without any swirl component. The inlet flow condition to the runner was determined by the three-dimensional flow analysis results from the wicket gates section. The solid lines in Fig. 2 show the meridional streamlines obtained by the three-dimensional flow analysis at the same operating point as that of Fig. 1. The dotted lines in the same Figure show the geometrical lines which equally divide the sectional area of meridional flow passage into eight.

The runner blade surface

The static pressure distribution on the low pressure surface of each runner blade was obtained (by the above analysis) to investigate the tendency of cavitation, occurring first at the point of minimum pressure. Fig. 3 shows the calculation result at the same operating point as Fig. 2. The abscissae show the length (L) along a blade from the leading edge, non-dimensionalized with the total length of the blade. Also, the ordinate is the static pressure coefficient, Cp, acting on the blade surface with respect to the total pressure at the outlet of runner blade and non-dimensionalized with the net head. Cp is defined as follows:

$$\begin{aligned} Cp &\equiv (p/\gamma - P_{TZ}/\gamma)/H \\ &\fallingdotseq \{p/\gamma - (-Hs + vd^2/2g)\}/H \end{aligned} \quad \ldots (1)$$

where:

p/γ : static pressure head on blade surface (mAq, at atmospheric pressure)
P_{TZ}/γ : total head at runner outlet (mAq, at atmospheric pressure)
H : net head (mAq)
Hs : suction head (mAq)
$vd^2/2g$: velocity head at draft tube outlet (mAq)

If the cavitation starts on the blade where the minimum static pressure, p_{min}, reaches the vapour pressure head of water, $Hv - Ha$ (mAq, at atmospheric pressure), Cp_{min} can be defined as follows:

$$\begin{aligned} Cp_{min} &\equiv \{p_{min}/\gamma - (P_{TZ}/\gamma)_{beg}\}/H \\ &\fallingdotseq \{(Hv - Ha) - (-Hs + vd^2/2g)_{beg}\}/H \\ &\equiv -\sigma_{beg} \end{aligned} \quad \ldots (2)$$

Ha : atmospheric pressure head (mAq)

Therefore, the incipient cavitation factor, σ_{beg}, can be obtained by acquiring the minimum pressure coefficient on the blade surface, Cp_{min}, from Fig. 3 and reversing the sign.

Fig. 3 shows the surface pressure distributions along the hub-, mid- and tip streamline of a blade, while the reference elevation is kept at the top of the runner. From the Figure, it is clear that the cavitation along the low pressure surface (l.p.s.) of the tip will start under the highest cavitation factor. When the installation cavitation factor is lowered, the cavitation occurs along the hub, then along the mid-streamline. The pressure along the hub reaches its minimum at approximately $L=0.5$. This is because the meridional flow velocity increases around the centre of the hub disk where the curvature of the hub contour is large, which results in the lowering of the static pressure (see Fig. 2).

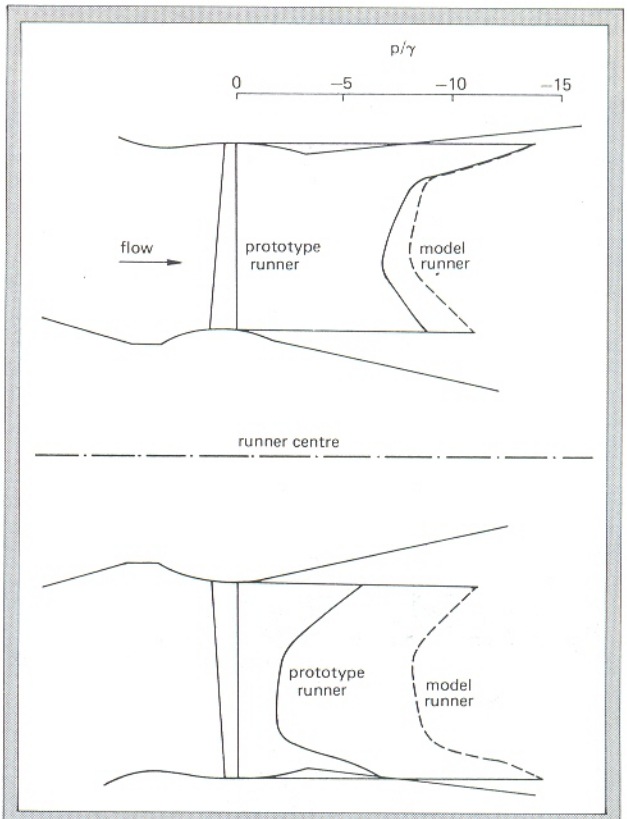

Fig. 4. The vertical distribution of the minimum pressure on the low pressure surface of the runner blades.

Evaluation of prototype cavitation characteristics

Distribution of cavitation

Fig. 4 shows the vertical distribution of minimum pressure on the low pressure surface of the blades obtained with the three-dimensional flow analysis. The dashed line shows the minimum pressure distribution of the model runner. The solid line, on the other hand, shows the minimum pressure distribution of the prototype runner. It is clear from the solid line that the pressure increases rapidly when a runner blade rotates from the top to the bottom.

Fig. 5 shows the vertical distribution of cavitation in the prototype runner which is obtained from the visual observation of the model cavitation test, while considering the prototype's minimum pressure distribution (as shown in Fig. 4). Fig. 5 shows that the cavitation development of the prototype at each elevation under the constant suction head can be quantitatively assumed from the observation result of the model. Therefore, to convert the model cavitation characteristics to that of the prototype, the above vertical distribution of cavitation development in the prototype runner at each elevation (per revolution) must be taken into consideration.

Conversion from model to prototype

To convert the cavitation characteristics of the model bulb turbine to the prototype, eight points (which have equal circumferential distance along the runner periphery and five different elevations, as shown in Fig. 5) are set from the runner top to bottom under an arbitrary, but constant, suction head. The unit output of the model at the respective cavitation factor, which corresponds to each of these five elevations, is obtained from Fig. 1. By taking the weighted mean of each unit output of the model, the output of the prototype is obtained. The weight for unit output is 1/8 at the runner top and bottom, and 1/4 for the other three elevations. This is because the runner will pass through the three intermediate elevations twice while the runner rotates once.

Fig. 6 shows the conversion to the prototype of the model cavitation characteristics shown in Fig. 1, derived by using the above method. This indicates that in the prototype cavitation characteristics, the decrease of output power becomes very gradual in the region below the critical sigma. Therefore, the value of sigma, $\sigma 1$, at the point where η deteriorates by 1 per cent, for example, seems quite pessimistic from the model characteristics, but actually there will be almost no cavitation problems.

Conclusion

By applying the results of three-dimensional flow analysis and the visual observation of model tests, the method described above can be established to convert the model cavitation characteristics of the prototype, allowing for the vertical distribution of cavitation in large low head bulb turbine runners.

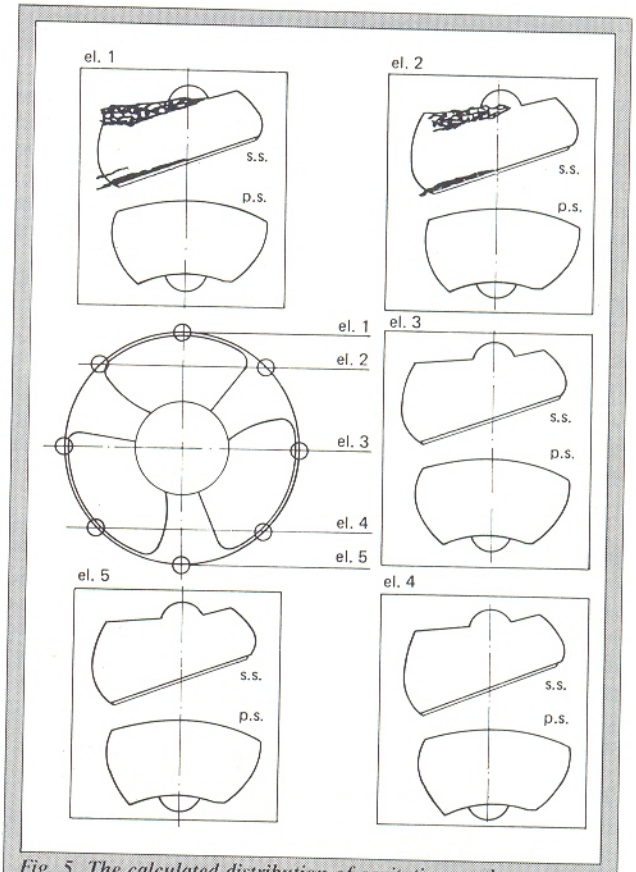

Fig. 5. The calculated distribution of cavitation on the prototype runner for the New Martinsville powerplant.

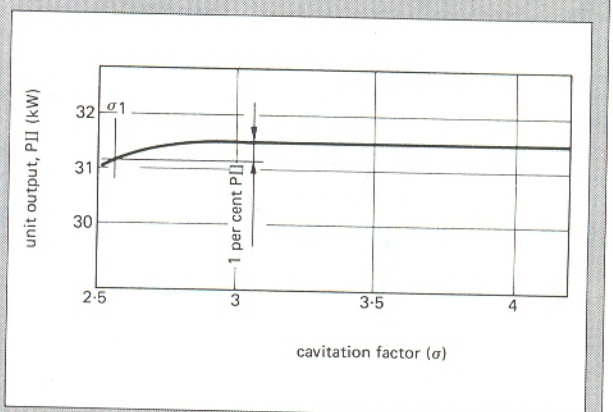

Fig. 6. The calculated cavitation/performance behaviour of the prototype, converted from the cavitation characteristics displayed by the model and the three-dimensional flow analysis.

References

1. IEC Model Test Code, First Supplement to Publication 193; 1965.
2. SAITO, J., YANO, M. AND ABE, A., *Fuji Electric Journal* (in Japanese), Vol. 60, No. 5; 1987.
3. KUBOTA, T., TAKIMOTO, S. AND AOKI, H., *Fuji Electric Review*, Vol. 23, No. 2; 1977.
4. SENOO, Y. AND NAKASE, Y., *Transcriptions* ASME, Series A, Vol. 93, No 4; 1971.
5. NAKASE, Y., SENOO, Y., *Transcriptions* ASME, Series A, Vol. 94, No. 1; 1972.